

SPECT Imaging With Resolution Recovery

Andrei V. Bronnikov

Abstract—Single-photon emission computed tomography (SPECT) is a method of choice for imaging spatial distributions of radioisotopes. Applications of this method are found in medicine, biomedical research and nuclear industry. This paper deals with improving spatial resolution in SPECT by applying correction for the point-spread function (PSF) in the reconstruction algorithm and optimizing the collimator. Several approaches are considered: the use of a depth-dependent PSF model for a parallel-beam collimator derived from experimental data, the extension of this model to a fan-beam collimator, a triangular approximation of the PSF for reconstruction acceleration, and a method for optimal fan-beam collimator design. An unmatched projector/back-projector ordered subsets expectation maximization (OSEM) algorithm is used for image reconstruction. Experimental results with simulated and physical phantom data of a micro-SPECT system show a significant improvement of spatial resolution with the proposed methods.

Index Terms—Image quality, nuclear medicine, single photon emission computed tomography (SPECT).

I. INTRODUCTION

SINGLE-PHOTON emission computed tomography (SPECT) is a method of choice for imaging spatial distributions of radioisotopes. Nice applications of this method exist in various fields ranging from nuclear medicine and biomedical research to nuclear industry. Intense research has been done and is still going on in the field of SPECT instrumentation and data processing. A comprehensive overview of state-of-the-art methods and applications can be found in [1]. Certain aspects of 3-D image reconstruction and attenuation correction in SPECT have been addressed by the author in [2], [3]. This paper deals with improving spatial resolution of the images. Similar approaches have been previously reported in [4]–[17]. The goal of our study was to demonstrate the ultimate resolution which can be achieved with any given SPECT system by using mathematical correction for the point-spread function (PSF) in the reconstruction algorithm and optimizing the collimator. In particular, we consider the use of a fan-beam collimator and provide a method for optimal fan-beam collimator design based on the experimentally measured PSF model of a parallel-beam collimator. Active research in collimator design was done in the 90s when basic principles of system characterization and analysis were proposed [4]–[6]. In this paper we make use of the results presented in [6] for the formula of a Van Mellekom fan-beam collimator and compare the numerical results obtained by this formula with new results obtained by

Manuscript received July 22, 2011; revised November 21, 2011; accepted April 04, 2012. Date of publication May 25, 2012; date of current version August 14, 2012.

The author is with Bronnikov Algorithms, 6800AB Arnhem, The Netherlands (e-mail: info@bronnikov-algorithms.com).

Color versions of one or more of the figures in this paper are available online at <http://ieeexplore.ieee.org>.

Digital Object Identifier 10.1109/TNS.2012.2195675

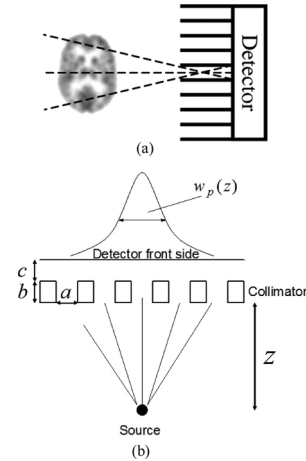


Fig. 1. SPECT collimation: (a) spatial resolution decreases with the distance; (b) PSF and geometrical parameters of the parallel-beam collimator.

the extension of the parallel-beam collimator model to the fan-beam collimator. Our parallel-beam collimator model is derived from experimental data obtained with a point source; we study both parallel-beam and fan-beam models using the formalism of a depth-dependent PSF. Correction for the PSF is done by application of the ordered subsets expectation maximization (OSEM) iterative algorithm. The basic formulation of this algorithm was suggested and studied in [9], [10]. The idea of using an unmatched projector/backprojector pair was first explored in [11], where it was shown that the use of the unmatched algorithms for forward and back projection leads to good results in resolution recovery while saving computational time. We expand this idea by resorting to a simplified approximation of the PSF which allows us to further decrease the computation cost. The proposed approach is universal and can be used with data acquired with any type of collimators, including parallel-beam, fan-beam, cone-beam, multihole and pinhole collimators – all of which are in the focus of active research during the last decade [12]–[16]. Experimental results obtained with a physical phantom demonstrate high efficiency of resolution recovery by the suggested approach and are in agreement with the results recently obtained by other approaches [17]. The method can be used in diverse applications including inspection of nuclear materials, medical imaging, and biomedical research.

II. METHODS

A. Point-Spread Function

In SPECT imaging, the photons emitted from the object are detected over a certain area behind the collimator (Fig. 1). The distribution of photons is characterized by a function called the “point-spread function” (PSF) of the system. The PSF can be

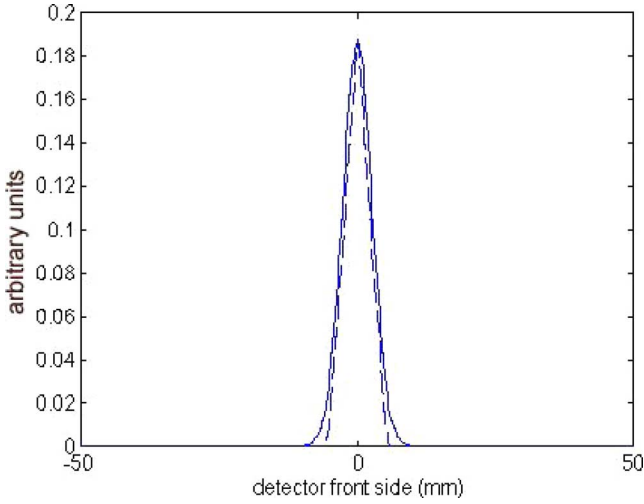


Fig. 2. Triangular approximation of the PSF at certain distance z .

measured by using a relatively small point source. Changing the position of the point source and acquiring the corresponding image at the pixel array, a set of 2D data describing the distance-dependent PSF can be collected. The measured PSF can then be fitted with a modeling function. Usually, the measured PSF of a SPECT system is fitted with a Gaussian distribution function

$$h_{z,\rho}(x) = \sqrt{\frac{2}{\pi}} \frac{1}{k(\rho) \times w_p(z)} \exp\left(\frac{-2x^2}{[k(\rho) \times w_p(z)]^2}\right) \quad (1)$$

where x is the position on the detector. Function $w_p(z)$ describes the width of the parallel-beam PSF dependent on the distance z of the point source to the collimator. Function $k(\rho)$ describes resolution degradation observed in the projection image at the radius ρ from the geometric center of the image. We use data obtained with a typical micro-SPECT system comprising a rotating gamma camera, a parallel-beam collimator and an animal holder. Making experiments with a point source at different locations, it was shown for this system that the width function for a 35/1.7 mm collimator can be fitted with a linear function

$$w_p(z) = 0.0356 \times z + 2.3827 \quad (2)$$

while function $k(\rho)$ has been determined as

$$k(\rho) = \begin{cases} 1.0, & \text{if } \rho < 33 \\ 0.0767 \times \rho - 1.5511, & \text{otherwise} \end{cases} \quad (3)$$

The PSF model (1) has one major drawback: computation of the Gaussian function at each step of the algorithm can be inefficient for high-resolution data. We suggest the replacement of function (1) by a nearby function that is faster to compute. For instance, function

$$h_{z,\rho}(x) = \begin{cases} \sqrt{\frac{2}{\pi}} \frac{1}{k(\rho) \times w_p(z)} \left(1 - \frac{|x|}{k(\rho) \times w_p(z)}\right), & \text{if } |x| \leq k(\rho) \times w_p(z) \\ 0, & \text{otherwise} \end{cases} \quad (4)$$

approximates the main part of the Gaussian PSF quite well (see Fig. 2) and can be computed much faster.

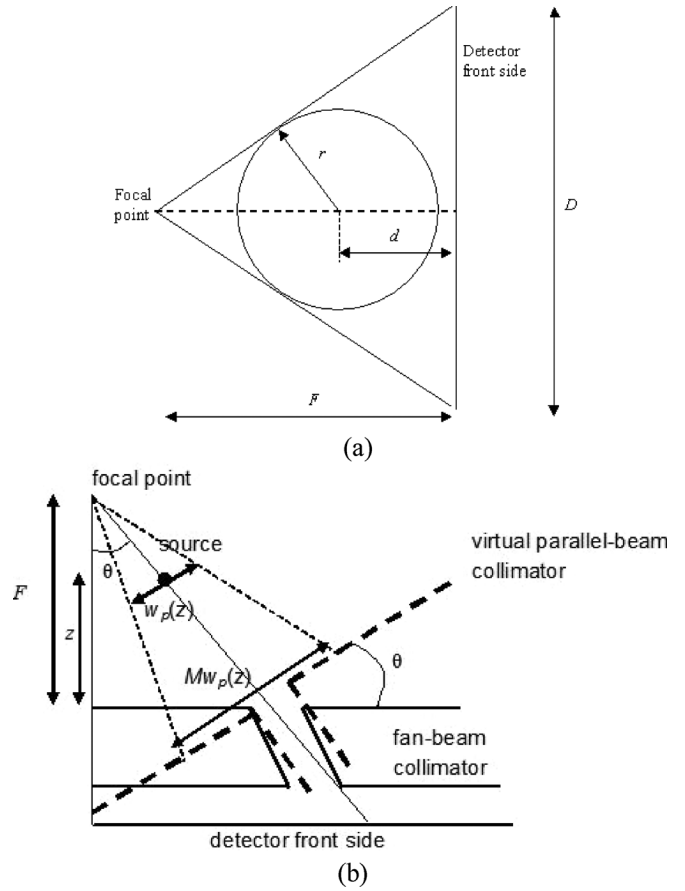


Fig. 3. Fan-beam collimation. (a) Geometry. (b) Derivation of (8).

B. Fan-Beam Collimation

It is a well-established fact that application of a converging collimator improves sensitivity and the signal-to-noise ratio. Let us consider the fan beam geometry shown in Fig. 3. The field of view is a cylinder the radius r . We assume that the field of view is fully covered by the fan beam and the following constrain holds:

$$r \leq d < \frac{D}{2}. \quad (5)$$

For given r , d and D , the shortest focal length can be found as

$$F = \frac{dD^2 + rD\sqrt{D^2 + 4(d^2 - r^2)}}{D^2 - 4r^2}. \quad (6)$$

The structures at the distance z from the detector are magnified with a factor

$$M = \frac{F}{F - z}. \quad (7)$$

Note that $F = \infty$ and $M = 1$ if $r = D/2$ (parallel beam geometry), whereas $M > 1$ for any $r < D/2$, which defines the case of the fan beam.

We cannot measure the PSF of the collimator that yet to be designed, so that other methods have to be used. For instance, these can be the following methods:

- derivation of the fan-beam PSF from the measured parallel-beam PSF;

— calculation of the geometrical response via analytical relationships.

To derive a relationship between the parallel-beam and fan-beam PSF, let us imagine that the hole of the fan-beam collimator is replaced by the hole of a virtual parallel-beam collimator in the same location. The width of the parallel-beam PSF will be magnified due to the geometrical magnification provided by the fan beam. Fig. 3(a) shows that the PSF width of the fan-beam collimator will be equal to

$$w_f(z) = \frac{M}{\cos\theta} w_p(z). \quad (8)$$

Since the PSF width $w_p(z)$ of the parallel-beam system is known from (2), the corresponding fan-beam PSF can easily be computed.

Another way to determine $w_f(z)$ is to derive it from geometrical relations. Several analytical methods for modeling fan-beam collimators were suggested in the literature [4]–[6]. All these methods require the knowledge of the design parameters of the collimator. Recently, a useful formula was derived and tested with experimental data obtained from a Van Mullekom fan-beam collimator [6]. In our notation this formula is written as

$$w_f(z) = \left(k_1 \frac{a(z+b+c)(2F+b)}{\sqrt{b^2(F-z)^2 - a^2(b+2z)^2}} + k_2 \right) \times \frac{1}{\cos\theta} \quad (9)$$

where parameters k_1 and k_2 have to be found by fitting with the measured PSF; geometrical parameters a, b, c are explained in Fig. 1. To use this formula with the parameters of our system, we have to find such k_1 and k_2 that fit (9) with (2) for the case of the parallel-beam geometry. Setting $F \rightarrow \infty$ and using parameters of the parallel-beam collimator (see Table I) we find $k_1 = 0.3665$ and $k_2 = 1.1367$. Equation (9) with given k_1 and k_2 can then be applied to determine the width of the fan-beam PSF for arbitrary F . The results of both approaches are compared in Fig. 4. The widths of the fan-beam PSF computed with (8) and (9) for $F = 100$ mm and the lateral position $x = 20$ mm of the source. Fig. 4 shows that both methods are in good agreement with each other, which leads us to the conclusion that both approaches are valid and can be applied in our situation. We will use (8) in the computations.

C. Correction for the PSF

The results of the previous section show that the fan-beam PSF can have a significant width, which will require application of special correction techniques for resolution recovery. Here we consider one possible method based on the OSEM reconstruction algorithm. A mathematical model of SPECT imaging can be written in the form

$$g_i \text{ is the realization of a Poisson variate } G_i \\ \text{with the mean } \bar{G}_i = \sum_j h_{ij} f_j \quad (10)$$

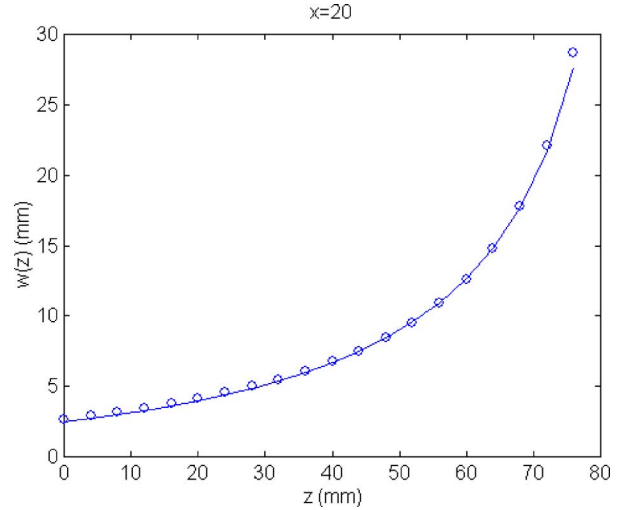


Fig. 4. Fan-beam PSF width computed with the use of the measured parallel-beam PSF (the solid line) and the analytical formula (circles).

TABLE I
PARAMETERS OF THE PARALLEL-BEAM COLLIMATOR

Parameter	Value (mm)
Diameter of the hole	1.7
Length	35
Clearance	0
Field of view	100 × 100

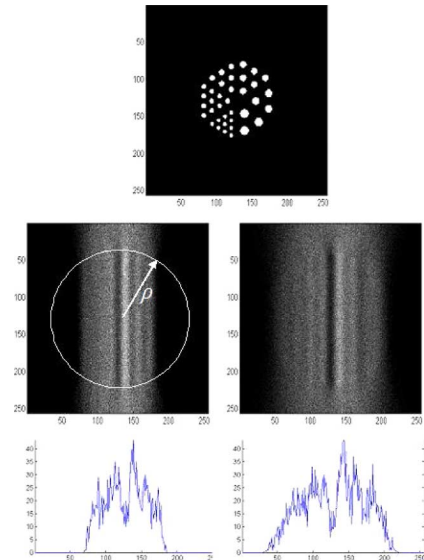


Fig. 5. Parallel and fan beam projections of the computer phantom (image degradation outside the circle with radius $\rho = 33$ mm is visible).

where g_i is the value of the i th detector bin, h is the PSF and f is the digital image represented by a set of voxels. The solvability of the inverse problem for (10) is strongly determined by the PSF. Since h is shift variant, application of deconvolution is impossible. However, function f can be reconstructed from (10) by the iterative OSEM algorithm using the PSF at the reprojection step. In such a way, the reconstructed image will be corrected

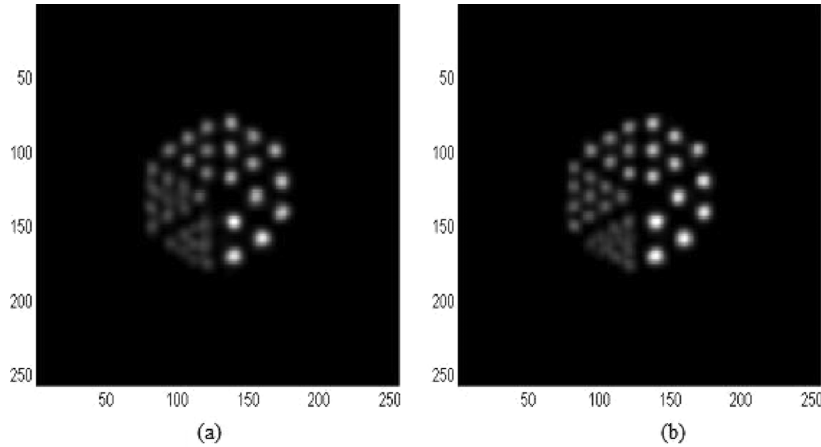


Fig. 6. Reconstruction of the computer phantom (256×256 pixels). (a) Parallel-beam reconstruction. (b) Fan-beam reconstruction. Twelve iterations of the OSEM algorithm with correction for the PSF have been done.

for the effects of the PSF. The algorithm for reconstruction of parallel-beam and fan-beam data is written as

$$f_j^{k,n} = f_j^{k,n-1} \frac{1}{\sum_{i \in S(n)} b_{ij}} \sum_{i \in S(n)} \frac{b_{ij} g_i}{\sum_j h_{ij} f_j^{k,n-1}} \quad (11)$$

where $S(n)$ is the n th subset of projections, h_{ij} is the PSF and b_{ij} is the probability that a photon emitted from pixel j is detected in the i th detector bin (the system matrix). Such an approach is called “unmatched projector/backprojector,” since the projector and backprojector operators are different here (see, e.g., [11]). Note that the probability function can be chosen in such a way that $\sum_{i \in S(n)} b_{ij} = N$, where N is the number of views per subset, which simplifies computations. In our approach, values $0 < b_{ij} \leq 1$ were computed as the coefficients of the linear interpolation between the adjacent detector bins. Equation (11) can also be used for reconstruction without compensation for the PSF by setting $h_{ij} = b_{ij}$. For sufficiently large widths of the PSF the inverse problem considered is severely ill-posed, that is relatively small variations in the data cause large errors in the solution. Special methods for stabilizing the solution are required. The most convenient way to stabilize the OSEM algorithm against the noise is to use a stopping criterion for the number of iterations and apply pre- and post-processing filtering. The Gaussian function is a fine choice for the filter function.

III. RESULTS

A. Computer Phantom Studies

In this section we consider a study of a computer phantom simulating small hot rods of different diameters. A dedicated software tool has been developed to compute parallel and fan-beam SPECT projections of the mathematical phantom using the PSF given by (2)–(4). These projections were used as the mean value of the Poisson data according to (10). A software tool that is a part of a standard mathematical library was applied to generate the Poisson statistics. The phantom was computed on the 3-D grid of $256 \times 256 \times 256$ voxels; 256 projections over

360 degrees with resolution 256×256 pixels were simulated. To compute the fan-beam projections, we have to specify the field of view. Let us first set in our study $D = 100$ mm, $r = 30$ mm and $d = 35$ mm. Inserting the values of D , r and d into (6) we find that the shortest focal distance for this field of view would be $F = 104$ mm. Realistic simulations have been done by application of the entire model (10) including the Poisson statistics. Fig. 5 shows the corresponding projections and their profiles after application of the Poisson algorithm. The number of counts is similar to that of a typical physical phantom. The smaller details in the projections are covered by noise. Fig. 6 shows the results of reconstruction of these data by applying (11). 12 iterations of the OSEM algorithm with correction for the PSF were done; the minimum of the residual functional (a squared norm of the difference between actual and recalculated projections) was used as the stopping rule. A Gaussian filter with the width of 10 pixels was applied both to the projection data and the final reconstructed image. Subsets of equal size were used; the number of projections per subset was chosen on the basis of the best image quality. Fig. 6 allows us to observe the effects of using a fan-beam collimator: contrast of the image reconstructed from the fan-beam data is better. There is also a certain improvement in resolution: the 2.5 mm rods are resolved better with the use of the fan beam. The 2 mm rods remain unresolved in both cases.

In the next experiment we have studied the influence of the geometrical efficiency of the fan beam. More efficient collimation can be achieved by minimizing the field of view. Let us set $r = 25$ mm and $d = 25$ mm. The focal distance for these parameters was found to be $F = 66$ mm. The largest magnification is provided here. The projections and the reconstruction are presented in Fig. 7. As seen from Fig. 7, the projection covers the entire detector. Correction for the PSF makes it possible to observe the smallest 2 mm rods. This is the ultimate result that can be achieved for this object with the given parameters of the fan beam.

B. Physical Phantom Studies

An experimental data set contained 256 parallel-beam projections with resolution of 256×256 pixels. Fig. 8 shows the first

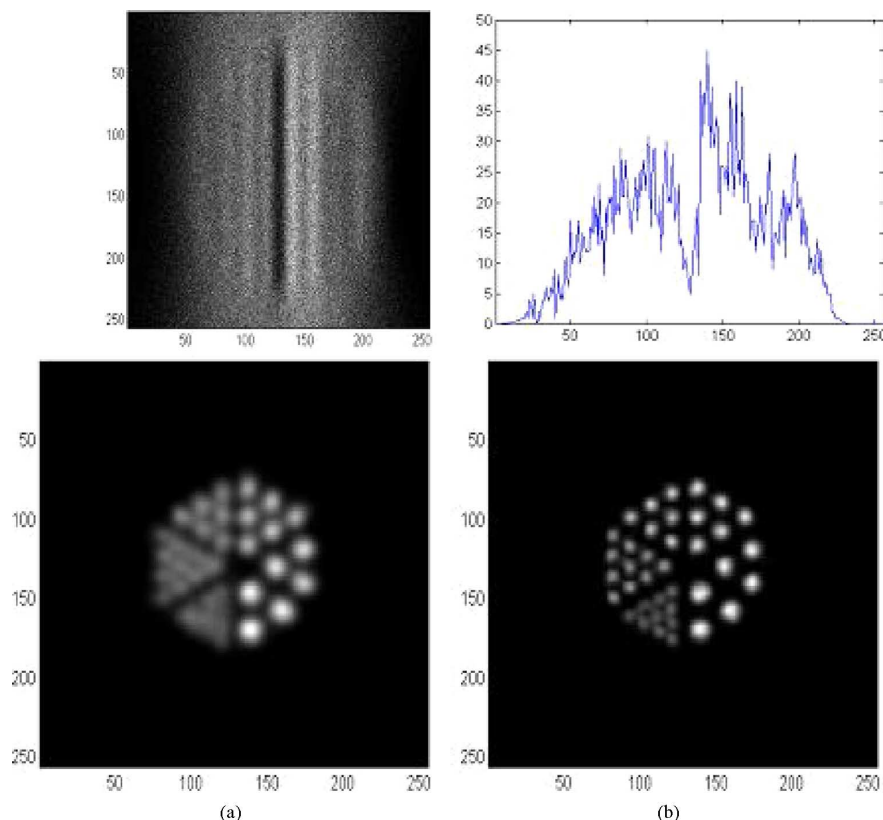


Fig. 7. Fan-beam projection computed with $r = d = 25$ mm, $F = 66$ mm. The best possible geometrical efficiency is achieved. Reconstruction of the computer phantom (a) no correction for the PSF and (b) with correction for the PSF.

projection from the data set. It is seen that the projections are quite noisy. The 35/1.7 collimator has better efficiency, which ensures larger average values of the projection. In this case, the number of counts is similar to that used in the computer simulations discussed in the previous section. Reconstruction of the hot rod data with and without correction for the PSF are shown in Fig. 8. Here we can see the dramatic improvement of the image quality and resolution provided by application of correction for the PSF. 12 iterations of the OSEM algorithm with correction for the PSF were made. A Gaussian filter with the pixel width of 10 pixels was applied both to the projection data and the reconstructed image. It is seen in Fig. 8 that the smallest 2 mm rods were resolved in the reconstruction after applying correction for the PSF. Larger rods have homogeneous contrast and are clearly visible. The profiles across the images demonstrate the improvement in quantification after correction for the PSF.

IV. DISCUSSION AND PRACTICAL CONSIDERATIONS

The experiments considered in the previous section show the advantage of using correction for the PSF in SPECT reconstruction. However, the application of this method has the problem of slowing the computations:

- more computations per iteration are needed because the width of the PSF is larger than the width of the interpolating function used in the algorithm without correction;
- more iterations of the OSEM algorithm are needed because of worse conditioning of the matrix based on the PSF model.

The computation time per iteration can be reduced by faster computation of the PSF. We suggest the use of a triangular PSF (4) that approximates the original Gaussian PSF, but is computed much faster. Note that the triangular PSF cuts off the nonzero side-lobes of the Gaussian function, but those long side-lobes may not be required at all when computing the unmatched projection/backprojection pair. The experiments showed that computation of a single step of the algorithm based on using the triangular PSF was three times faster than computation of the same step using the Gaussian PSF. The method of over relaxation can be used to further accelerate the OSEM algorithm [7], [8]. Acceleration in three times without significant loss of quality was also reported in [7]. Other approaches include the use of a better initial approximation, e.g., the image reconstructed by a filtered backprojection technique. Acceleration can also be achieved by reducing the time per iteration. This can be done by using different kernels at the reprojection and backprojection steps. The use of a 1-st order interpolation kernel at the backprojection step reduces the computation time significantly.

The geometrical design of the collimator is another important issue. One of the main geometrical parameters of the fan-beam collimator is the focal distance. We suggest a method of finding the shortest focal distance for a given field of view. The shortest focal distance provides the best results in terms of geometrical efficiency. We assume that the field of view is defined by a cylinder specified by its radius and height. The center of the field of view is set on a certain distance from the collimator front

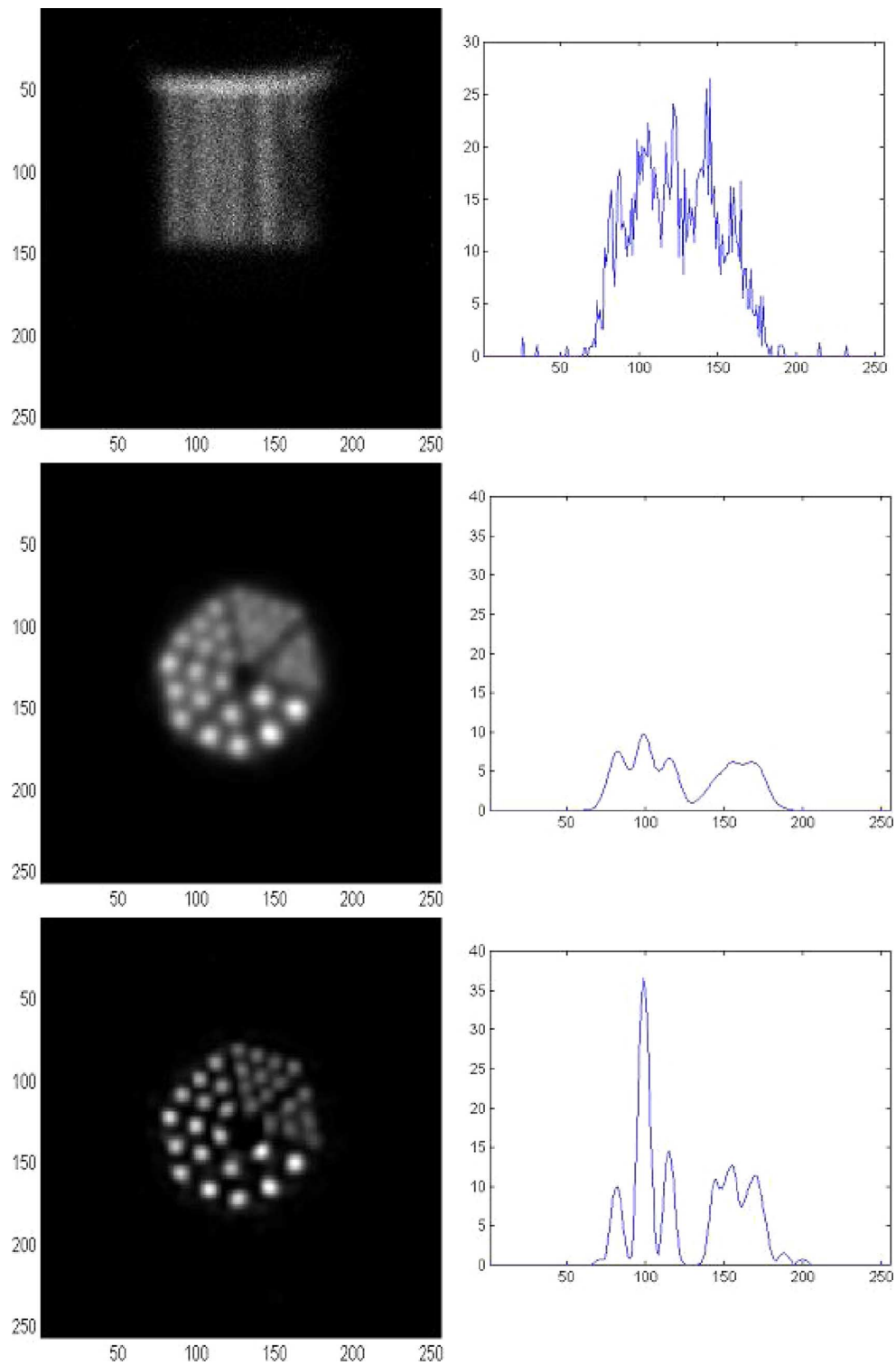


Fig. 8. Reconstruction of a physical phantom. Upper row: a projection. Middle row: reconstruction without correction for the PSF. Lower row: resolution recovery with correction for the distance-dependent PSF.

side. In this case, the shortest focal distance can be found by formula (6). The experiments have showed that the image quality improves for the smaller fields of view, where shorter focal distances are used. The field of view is here a cylinder with the radius of 20 mm and the height of 100 mm. The center of the field of view is 21 mm away from the collimator. This geom-

etry ensures at least 1 mm clearance between the object and the detector and determines the focal distance of 100 mm for the 35 mm collimator. Theoretically, the fan-beam collimator designed will have the PSF width satisfying (8). For the “prototype” parallel-beam collimator the parameters from Table I can be used.

V. SUMMARY

Two methods for resolution recovery in SPECT imaging have been studied: correction for the distance-dependent PSF and the use of a fan-beam collimator. An unmatched projector/backprojector OSEM reconstruction algorithm employing the PSF at the reprojection step has been developed and implemented for both parallel-beam and fan-beam configurations. A fast implementation of the OSEM algorithm using a triangular approximation to the measured PSF has been made. Extension of a parallel-beam model to the fan-beam collimator model has been done; two different approaches of doing this have been compared. Computer and physical phantom studies have been carried out. It was demonstrated that simultaneous application of a fan-beam collimator and correction for the PSF leads to the best results in resolution recovery.

REFERENCES

- [1] M. Wenick and J. Aarsvold, *Emission Tomography: The Fundamentals of PET and SPECT*. New York: Elsevier, 2004.
- [2] A. V. Bronnikov, "A filtering approach to image reconstruction in 3D SPECT," *Phys. Med. Biolog.*, vol. 45, pp. 2639–2651, 2000.
- [3] A. V. Bronnikov, "Reconstruction of attenuation map using discrete consistency conditions," *IEEE Trans. Med. Imag.*, vol. 19, no. 5, pp. 451–62, May 2000.
- [4] B. M. W. Tsui and G. T. Gullberg, "The geometric transfer function for cone and fan beam collimators," *Phys. Med. Biol.*, vol. 35, pp. 81–93, 1990.
- [5] A. R. Formiconi, "Geometrical response of multihole collimators," *Phys. Med. Biolog.*, vol. 43, pp. 3359–3379, 1998.
- [6] D. Pareto, J. Pavia, C. Falcon, I. Juvellis, A. Cot, and D. Ros, "Characterisation of fan-beam collimators," *Eur. J. Nucl. Med.*, vol. 28, no. 2, pp. 144–149, 2001.
- [7] R. M. Lewitt and G. Muehllehler, "Accelerated iterative reconstruction for positron emission tomography based on the EM algorithm for maximum likelihood estimation," *IEEE Trans. Med. Imag.*, vol. 5, no. 1, pp. 16–22, Jan. 1986.
- [8] P. Schmidlin, G. Brox, M. E. Belleman, and W. J. Lorentz, "Computation of high overrelaxation parameters in iterative image reconstruction," *IEEE Trans. Nucl. Sci.*, vol. 45, no. 3, pp. 1737–1742, Jun. 1998.
- [9] H. M. Hudson and R. S. Larkin, "Accelerated image reconstruction using ordered subsets of projection data," *IEEE Trans. Med. Imag.*, vol. 13, no. 4, pp. 601–609, Dec. 1994.
- [10] B. F. Hutton, H. M. Hudson, and F. J. Beekman, "A clinical perspective of accelerated statistical reconstruction," *Eur. J. Nucl. Med.*, vol. 24, pp. 797–808, 1997.
- [11] G. L. Zeng and G. Gullberg, "Unmatched projector/backprojector pairs in an iterative reconstruction algorithm," *IEEE Trans. Med. Imag.*, vol. 19, no. 5, pp. 548–55, May 2000.
- [12] N. U. Schramm, G. Ebel, U. Engeland, T. Schurrat, M. Behe, and T. M. Behr, "High-resolution SPECT using multipinhole collimation," *IEEE Trans. Nucl. Sci.*, vol. 50, no. 3, pp. 315–320, Jun. 2003.
- [13] F. J. Beekman and B. Vastenhouw, "Design and simulation of a high-resolution stationary SPECT system for small animals," *Phys. Med. Biol.*, vol. 49, no. 19, pp. 4579–4592, 2004.
- [14] A. Andreyev, M. Defrise, and C. Vanhove, "Pinhole SPECT reconstruction using blobs and resolution recovery," *IEEE Trans. Nucl. Sci.*, vol. 53, no. 5, pp. 2719–2728, Oct. 2006.
- [15] Y. C. Wang and B. M. W. Tsui, "Pinhole SPECT with different data acquisition geometries Usefulness of unified projection operators in homogeneous coordinates," *IEEE Trans. Med. Imag.*, vol. 26, no. 3, pp. 298–308, Mar. 2007.
- [16] K. Vunckx, J. Nuyts, B. Vanbilloen, M. De Saint-Hubert, D. Vanderghinste, D. Rattat, F. Mottaghy, and M. Defrise, "Optimized multipinhole design for mouse imaging," *IEEE Trans. Nucl. Sci.*, vol. 56, no. 5, pp. 2696–2705, Oct. 2009.
- [17] B. Zhang and G. L. Zeng, "High-resolution versus high-sensitivity SPECT imaging with geometric blurring compensation for various parallel-hole collimation geometries," *IEEE Trans. Inf. Technol. Biomed.*, vol. 14, no. 4, pp. 1121–7, Jul. 2010.